Journal of Applied Electrochemistry (2006) 36:599–602
DOI 10.1007/s10800-005-9112-9

Electrochemical behavior of anatase TiO_2 in aqueous lithium hydroxide electrolyte

MINAKSHI MANICKAM*, PRITAM SINGH, TOUMA B. ISSA and STEPHEN THURGATE
Division of Science and Engineering, Murdoch University, Murdoch, 6150, Western Australia
*(*author for correspondence, fax: + 61-8-9310-1711, e-mail: minakshi@murdoch.edu.au)*

Received 24 August 2005; accepted in revised form 14 December 2005

Key words: anatase, $LiTiO_2$, oxidation, reduction, TiO_2

Abstract

The electrochemical behavior of titanium dioxide (TiO_2) in aqueous lithium hydroxide (LiOH) electrolyte has been investigated. Cyclic voltammetry shows that electroreduction results in the formation of a number of products. X-ray diffraction of the electroreduced TiO_2 shows that Li_xTiO_2, Ti_2O_3, Ti_2O and TiO are formed. The formation of Li_xTiO_2 is confirmed through X-ray photoelectron spectroscopy (XPS) and Fourier transform infrared spectroscopy (FTIR) studies of the electroreduced TiO_2. The formation of Li_xTiO_2 is electro reversible. In this respect, the electrochemical behavior of TiO_2 in concentrated aqueous lithium hydroxide electrolyte is similar to that for lithium perchlorate ($LiClO_4$) non-aqueous media.

1. Introduction

In recent years much effort has been directed towards the development of renewable energy conversion and storage devices based on inexpensive materials. In this respect titanium dioxide (TiO_2) has attracted considerable academic and practical interest. Its semi conducting properties together with its chemical stability make it an excellent candidate for use in rechargeable batteries, electro chromic devices and solar cells. In particular, it has been extensively used in lithium ion batteries. It is due to its ability to accommodate small foreign ions, such as Li^+ and H^+ in its host structure through an intercalation process. Titanium dioxide exists in nature in various polymorphs [1] such as rutile (tetragonal), anatase (tetragonal) and brookite (orthorhombic). The rutile and anatase are the most thermodynamically stable phases and common forms of the TiO_2. These materials behave differently when used as cathodes in lithium cells. Ohzuku and Kodama [2] showed that diffusion of lithium into the TiO_2 (anatase) was easier than for rutile, because of different structural features. The electrochemical behavior of anatase TiO_2 in lithium ion non-aqueous electrolytes has been widely reported [3–6].

In non-aqueous lithium electrolytes, the following reaction for TiO_2 is generally written [2]

$$\square Ti^{4+}O^{2-} + xLi^+ + xe^- Li_xTi^{4+}_{1-x}Ti^{3+}_xO^{2-} \quad (1)$$

where $\square$ denotes vacant sites and x varies from 0.5 to 1, depending on the experimental techniques used.

Very little information on the electrochemical behavior of TiO_2 in aqueous media is available. Lyon and Hupp [7, 8] reported that the electrochemical reduction of TiO_2 involves irreversible (H^+) proton uptake (protonation) in aqueous H_2SO_4 or NaOH electrolytes. This proton intercalation mechanism was supported by electrochemical quartz crystal microbalance (EQCM) measurements. In this paper, we report our investigation of the reduction/oxidation (redox) behavior of TiO_2 (anatase) in an aqueous lithium hydroxide electrolyte and its comparison with that in non-aqueous lithium ion electrolytes. This work follows on our recent study of MnO_2 [9–11] where we reported that MnO_2 in aqueous lithium electrolytes behaved very similar to that in non-aqueous electrolytes.

2. Experimental

A list of the chemicals used in this study is given in Table 1. A standard three-electrode system was used for the cyclic voltammetric studies as shown in the Figure 1. The TiO_2 working electrode was made as follows: TiO_2 powder was pressed onto a disc of Pt gauze. On the other side of the disc, a layer of carbon was also pressed. The TiO_2 side of the disc (thickness of 1 mm) was exposed to the LiOH electrolyte through a Teflon barrel as shown in Figure 1. For making electrical connection of TiO_2 a Pt disc was inserted into the barrel on top of the carbon side which contacted stainless steel plunger. The counter electrode was a Zinc foil, which was separated from the main electrolyte by means of a

Table 1. List of chemicals

Chemical	Supplier	Grade (%)
TiO_2	Sigma-Aldrich	99.9
Zn foil	BDH chemicals	99.9
Lithium hydroxide monohydrate	Sigma chemicals	99.9
Zinc sulphate heptahydrate	Ajax chemicals	99.9

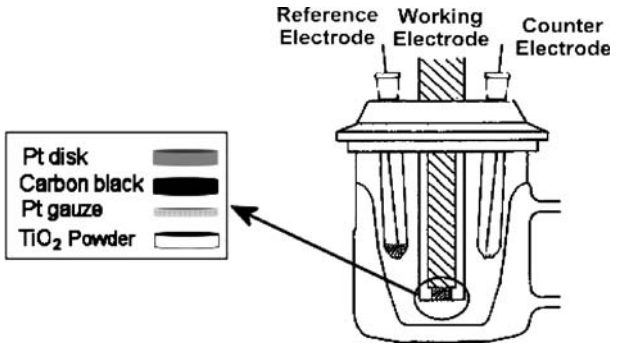

Fig. 1. Schematic diagram of a three cell system.

porous frit. A saturated calomel electrode (SCE) served as the reference electrode. The recorded values are reported as such. The electrolyte was a saturated (~5 molar) solution of lithium hydroxide. The working electrode was cycled between 0 and −0.6 V each time starting at 0 V going initially in the cathodic direction. An EG & G PAR Potentiostat/Galvanostat model 273 A, operated by model 270 software (EG&G) was used to scan at 25 $\mu V\ s^{-1}$ in all experiments.

The products formed during the electroreduction of TiO_2 were characterized by a Siemens X-ray diffractometer using Philips CoKα radiation. X-ray photoelectron spectroscope (Kratos Ultra Axis Spectrometer) was used to analyze the chemical binding energy of the samples using monochromatic AlKα (1486.6 eV) radiation. The X-ray photoelectron spectroscopy (XPS) analysis was started when the pressure in the analysis chamber fell below 1×10^{-9} hPa. Carbon, C (1s), was used as a reference for all the samples. The Fourier transform infrared spectrum (FTIR) was recorded using a Nicolet Magna-IR 850 spectrometer. For the FTIR study, TiO_2 was mixed thoroughly with KBr and for each sample an average of 16 scans were recorded.

3. Results and discussion

3.1. *Reduction/oxidation (redox) behavior of anatase TiO_2*

The redox behavior of the anatase TiO_2 was investigated voltammetrically by cycling in the potential region 0 to −0.6 V. Figure 2 shows one such cyclic voltammogram (CV). The cathodic portion of the scan consists of a series of peaks. The prominent peaks occur at potentials −396 and −496 mV. The reverse anodic scan consists of only one peak at −200 mV. This suggests that the reduction of TiO_2 occurs through more than one

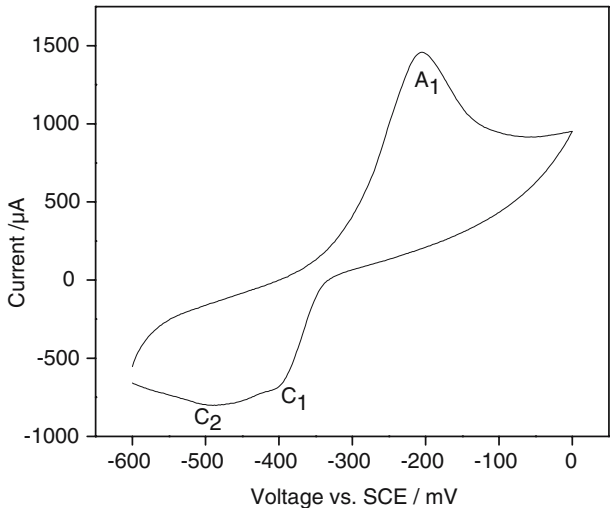

Fig. 2. Cyclic voltammogram of TiO_2 (scan rate: 25 μVs^{-1}).

mechanisms but only one reduction product undergoes reversible oxidation. The products of electroreduction of TiO_2 were identified by various techniques as discussed in the following section.

3.1.1. *X-ray diffraction*

Figure 3 shows the X-ray diffraction pattern of the material formed on scanning TiO_2 to −496 mV, the potential where reduction occurs. The X-ray diffraction pattern of the TiO_2 before the reduction experiment (Figure 3a) matches that of anatase TiO_2 having a tetragonal lattice with $a = 3.792$ Å and $c = 9.514$ Å. The material formed after the reduction scan (Figure 3b) shows new peaks at $2\theta = 36.1°$, 37.3°, 39.8°, 41.2° and 52.3° in addition to those present in the original material (Figure 3a). Based on the literature we assign the peak at $2\theta = 37.3°$ to Ti_2O_3 and those at 41.2° and 52.3° to Li_xTiO_2 [2, 12]. The peaks at $2\theta = 36.1°$ and 39.8° are assigned to Ti_2O and TiO, respectively. This indicates that the electroreduction of TiO_2 leads to the formation of intercalated TiO_2 (Li_xTiO_2), Ti_2O_3, Ti_2O and TiO. Since the ionic radius of Li^+ is almost identical to that of Ti^{3+} radii (~0.7 Å) the formation of lithium

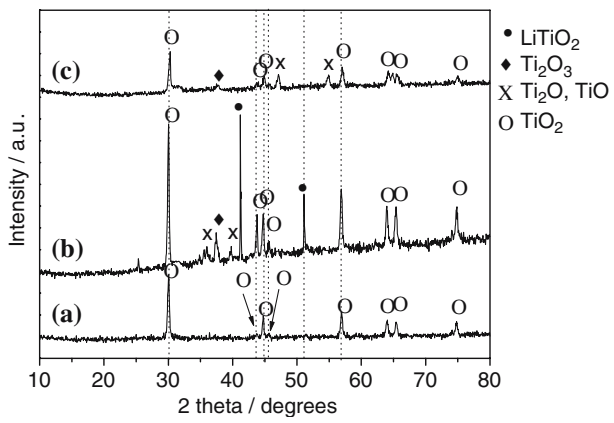

Fig. 3. X-ray diffraction patterns of titanium dioxide (TiO_2) (a) before reduction (b) after electroreduction at −496 mV and (c) after subsequent electrooxidation at −200 mV.

intercalated TiO_2 is reasonable. In this regard, the behavior of TiO_2 in aqueous LiOH electrolyte is similar to that in non-aqueous $LiClO_4$ electrolyte [2, 13–16]. However, the phases Ti_2O_3, TiO and Ti_2O are not seen in the non-aqueous systems, but, Lyon and Hupp [7] explained the formation of these reduced phases in aqueous system via irreversible proton intercalation. The XRD pattern of the material (Figure 3c) formed on subsequent oxidation at −200 mV does not contain the peaks at 41.2° and 52.3° indicating the Li_xTiO_2 reverts back to TiO_2. All the other peaks corresponding to TiO_2 remain unchanged. Thus the intercalation of TiO_2 to form $LiTiO_2$ is reversible.

3.1.2. *X-ray photoelectron spectroscopy*

Figure 4a shows the X-ray photoelectron spectra (XPS) of the TiO_2 before reduction at −496 mV. The symmetric Ti 2p peaks, indicate the material to be stoichiometric TiO_2 with a low concentration of defects. The spin-orbit splitting was 5.6 eV, with an intensity ratio of 0.26 between the Ti $2p_{1/2}$ and Ti $2p_{3/2}$. Figure 4b shows Ti (2p) peaks of the same material after electroreduction at the fifth scan. As can be seen in Figure 4b, a clear chemical shift of Ti (2p) towards lower binding energy is observed. This chemical shift reflects the change of Ti^{4+} to Ti^{3+} oxidation state. Ebina et al. [15] and Sodergren et al. [17] also observed a similar chemical shift of Ti (2p) when TiO_2 was electroreduced in non-aqueous $LiClO_4$ electrolyte indicating the formation of lithium intercalated TiO_2 phase (Li_xTiO_2).

Figure 5 shows the XPS spectra of the Li (1s) region of TiO_2 before and after electroreduction. For the unreduced sample no signal corresponding to Li (1s) is seen (Figure 5a), instead, only a satellite peak of Ti (3s) at 59.5 eV region occurs. The material after reduction (Figure 5b) contains a highly developed peak corresponding to Li (1s) at 55.1 eV [18]. To eliminate the possibility that the observed Li (1s) signal for the electroreduced sample was not just due to some lithium ion impurity such as Li_2CO_3 which could have been formed through the exposure of the TiO_2 to the electrolyte LiOH and atmospheric CO_2, the following experiment was done. The material after electroreduction was washed thoroughly with acetone several times until no further Li^+ ions were detected in the washing liquid. The resultant powder was dried and pressed back into a pellet and its XPS spectra recorded. As can be seen from Figure 6, the Li (1s) was still present suggesting that the material indeed was Li_xTiO_2. Chauvat et al. [19] have reported similar XPS data for the formation of Li_xTiO_2 in molten Li_2CO_3–Na_2CO_3 fuel cells.

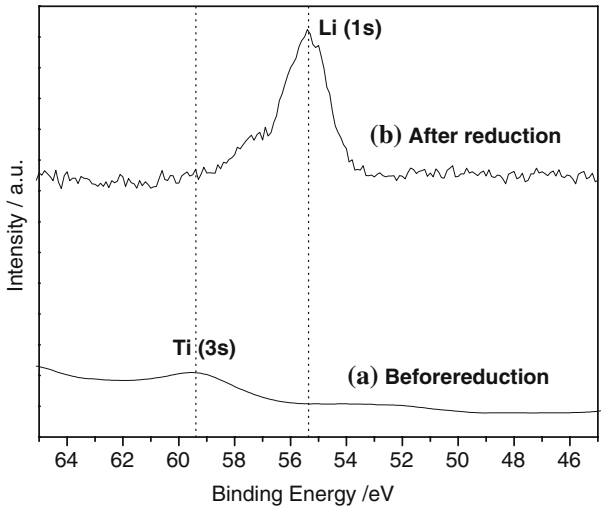

Fig. 5. XPS spectra of Ti (3s) and Li (1s) of the titanium dioxide (TiO_2): (a) before reduction and (b) after electroreduction at −496 mV.

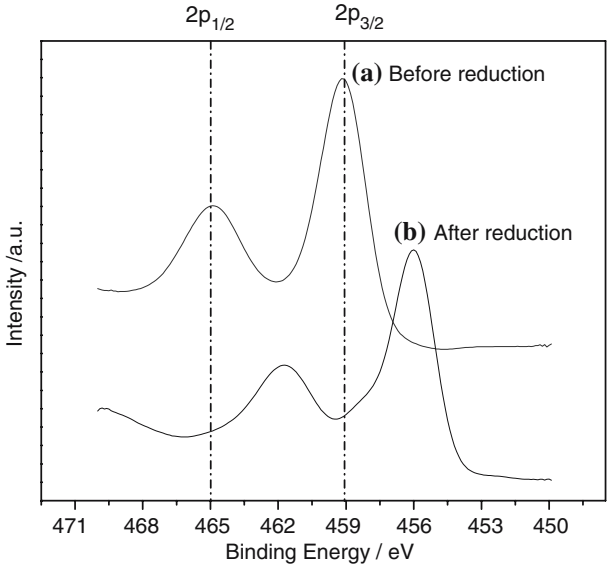

Fig. 4. XPS spectra of Ti 2p (3/2) and (1/2) of titanium dioxide (TiO_2): (a) before reduction and (b) after electroreduction at −496 mV.

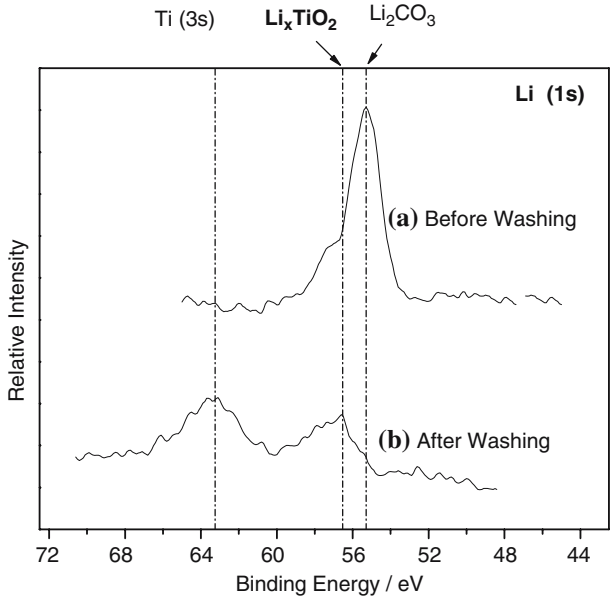

Fig. 6. The XPS spectra of Li (1s) of titanium dioxide (TiO_2) electroreduced at −496 mV: (a) before washing and (b) after washing with acetone.

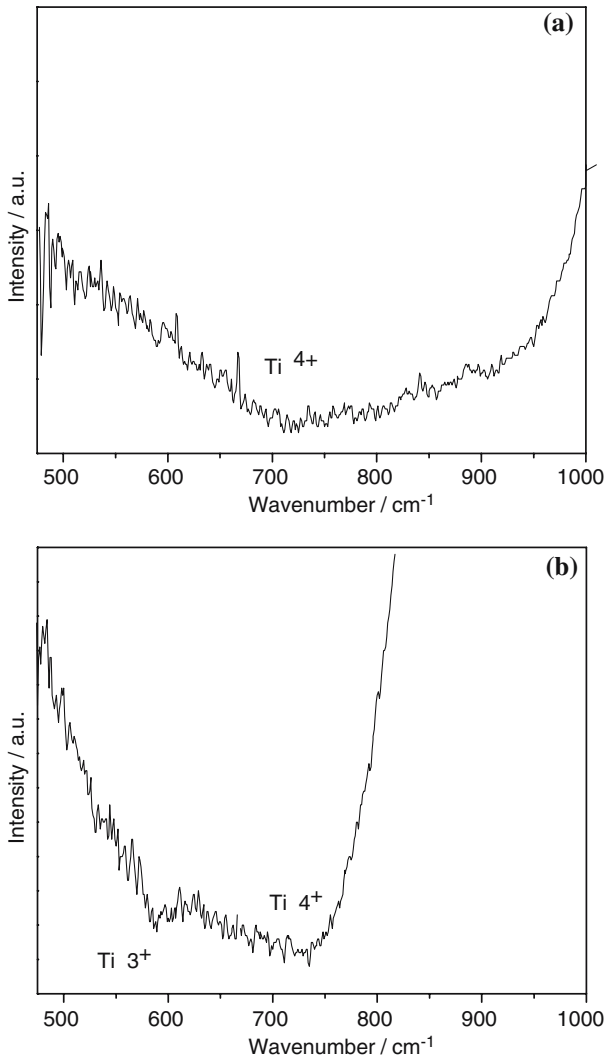

Fig. 7. FTIR spectra of titanium dioxide (TiO_2) cathode: (a) before and (b) after electroreduction at −496 mV.

3.1.3. *Infra-red spectra*

The infra-red spectra of TiO_2 material in the region 500–1000 cm^{-1} is shown in Figure 7. The broad peak at around 700 cm^{-1} for the material before the electroreduction, Figure 7a, corresponds to TiO_2 lattice vibration similar to that reported by Lee et al. [20]. The spectra for the same material after electroreduction have a new peak at 600 cm^{-1} (Figure 7b), similar spectra were observed for $LiTi_2O_4$ by Picquart et al. [21].

4. Conclusions

The electrochemical behavior of TiO_2 in a saturated aqueous LiOH electrolyte was investigated. It was found that reduction of TiO_2 in aqueous LiOH occurs forming a number of reduction products. Only one of these products can be reversibly oxidized. The X-ray diffraction (XRD) studies show that Li_xTiO_2 is the product which is reversibly formed during electroreduction/oxidation. Additionally, Ti_2O_3, Ti_2O and TiO phases are also formed which are not reversible. X-ray photoelectron spectroscopy (XPS) and Fourier-transform infrared (FTIR) spectral studies of the material confirm the formation of lithium intercalated TiO_2. This behavior of TiO_2 is found to be similar to that reported for lithium perchlorate ($LiClO_4$) non-aqueous electrolytes.

Acknowledgements

One of us (Minakshi Manickam) is grateful to Murdoch University for a research scholarship. The financial support of Australian Institute of Nuclear Science and Engineering (AINSE) to carry out some work at Australian Nuclear Science and Technology Organization (ANSTO) is also acknowledged. M. M thanks Doug Clark, Ken Seymour and Stewart Kelly of Murdoch University for their technical support in carrying out some of the experiments.

References

1. W.C. Mackrodt, *J. Solid State Chem.* **142** (1999) 428.
2. T. Ohzuku and T. Kodama, *J. Power Sources* **14** (1985) 153 and references stated therein.
3. S. Huang, L. Kavan, I. Exnar and M. Gratzel, *J. Electrochem. Soc.* **142** (1995) L142.
4. B. Zachau-Christiansen, K. West, T. Jacobsen and S. Atlung, *Solid State Ionics* **40–41** (1990) 580.
5. H. Kawamura, Y. Muranushi, T. Miura and T. Kishi, *Denki Kagaku* **59** (1991) 766.
6. D. Bi, J. Wang, Y. Sun and Z. Liao, *Proc. Workshop on Lithium Nonaqueous Battery Electrochemistry*, (The Electrochemical Society (Cleveland Section), NASA-LEWIS Res. Cent., and Case Institute of Tech., 1980), p. 130.
7. L.A. Lyon and J.T. Hupp, *J. Phys. Chem. B* **103** (1999) 4623.
8. L.A. Lyon and J.T. Hupp, *J. Phys. Chem. B* **99** (1995) 15718.
9. Manickam Minakshi, Pritam Singh, Touma B. Issa, Stephen Thurgate and Roland De Marco, *J. Power Sources* **130** (2004) 254.
10. Manickam Minakshi, Pritam Singh, Touma B. Issa, Stephen Thurgate and Roland De Marco, *J. Power Sources* **138** (2004) 319.
11. Manickam Minakshi, Pritam Singh, Touma B. Issa, Stephen Thurgate and Roland De Marco, *J. Power Sources* **153**(1) (2006) 165.
12. JCPDS cards: 16-223 and 10-63.
13. D.W. Murphy, M. Greenblatt, S.M. Zahurak, R.J. Cava, J.V. Waszczak, G.W. Hull Jr. and R.S. Hutton, *Rev. Chim. Miner.* **19** (1982) 441.
14. F. Bonino, L. Busani, M. Lazzari, M. Manstretta and B. Rivolta, *J. Power Sources* **6** (1981) 261.
15. T. Ebina, T. Iwasaki, Y. Onodera, H. Hayashi, T. Nagase, A. Chatterjee and K. Chiba, *J. Power Sources* **81–82** (1999) 393.
16. T. Ohzuku, Z. Takehara and S. Yoshizawa, *Electrochim. Acta* **24** (1979) 219.
17. S. Sodergren, H. Siegbahn, H. Rensmo, H. Lindstom, A. Hagfeldt and S.E. Lindquist, *J. Phys. Chem. B* **101** (1997) 3087.
18. Perkin Elmer Corporation, Handbook of X-ray Photoelectron Spectroscopy, Physical Electronics Division, Perkin Elmer Corporation, USA, October 1992.
19. V. Chauvat, E. Duval, B. Malinowska, M. Cassir and P. Marcus, *J. Mater. Sci.* **34** (1999) 2015.
20. S.J. Lee, S.W. Han, M. Yoon and K. Kim, *Vibration. Spectrosc.* **24** (2000) 265.
21. M. Picquart, L. Escobar-Alarcon, E. Torres, T. Lopez and E. Haro-Ponitowski, *J. Mater. Sci.* **37** (2002) 3241.